REPORT DOCUMENTATION PAGE	*Form Approved* *OMB No. 0704-0188*

1. REPORT DATE *(DD-MM-YYYY)*	2. REPORT TYPE	3. DATES COVERED *(From - To)*
14-02-2012	Conference Proceedings	

4. TITLE AND SUBTITLE
Measurements of Hurricane Induced High-Frequency Currents

5a. CONTRACT NUMBER

5b. GRANT NUMBER

5c. PROGRAM ELEMENT NUMBER
0601153N

6. AUTHOR(S)
Dianne Fribance, Hemantha Wijesekera, William Teague

5d. PROJECT NUMBER

5e. TASK NUMBER

5f. WORK UNIT NUMBER
73-4491-01-5

7. PERFORMING ORGANIZATION NAME(S) AND ADDRESS(ES)
Naval Research Laboratory
Oceanography Division
Stennis Space Center, MS 39529-5004

8. PERFORMING ORGANIZATION REPORT NUMBER
NRL/PP/7330-11-0769

9. SPONSORING/MONITORING AGENCY NAME(S) AND ADDRESS(ES)
Office of Naval Research
One Liberty Center
875 North Randolph Street, Suite 1425
Arlington, VA 22203-1995

10. SPONSOR/MONITOR'S ACRONYM(S)
ONR

11. SPONSOR/MONITOR'S REPORT NUMBER(S)

12. DISTRIBUTION/AVAILABILITY STATEMENT
Approved for public release, distribution is unlimited.

20120217350

13. SUPPLEMENTARY NOTES

14. ABSTRACT
Hurricanes are powerful, energetic storms that can be fueled by warm ocean waters, while simultaneously driving transport and mixing under their path. Wind-driven mixing is an important mechanism for generating internal waves, and hurricanes are capable of generating particularly high levels of mixing. The internal waves in turn allow diapycnal mixing in the ocean, accelerating heat transfer from the near surface to deeper waters. This plays a role in global thermohaline circulation, affecting heat transfer and therefore density properties throughout the oceans. However, while the importance of internal waves is well established, direct measurements of hurricane-generated internal waves over the shelf and slope regions are scarce. As a result, the mechanisms for the generation of these waves by storms are poorly understood. Here we examine the high frequency response and generation of internal waves by Hurricane Ivan as it travelled over the continental shelf edge and slope in the Gulf of Mexico. Velocity data were collected as part of the Naval Research Laboratory's Shelf Energetics and Exchange Dynamics (SEED) experiment. Moorings consisted of Trawl Resistant Bottom Mounts (TRBMs) in the form of a dome-shaped pod known as a Barny due to its barnacle-like shape. The Barnies housed ADCPs and wave/tide gauges, and during the hurricane were subject to extreme current conditions. In particular, over the shelf where water depths are 60 - 90m and surface waves reached significant wave heights of at least 20 m, bottom currents generated by these waves were over 2 m s^{-1}. Despite these extreme conditions, which set the nearby National Data Buoy Center (NDBC) buoy 42040 adrift, the Barnies proved themselves to be robust, and continued to measure water velocity and pressure both during and after the hurricane's presence in the region.

15. SUBJECT TERMS
high-frequency waves, dissipation,super-inertial

16. SECURITY CLASSIFICATION OF: a. REPORT	b. ABSTRACT	c. THIS PAGE	17. LIMITATION OF ABSTRACT	18. NUMBER OF PAGES	19a. NAME OF RESPONSIBLE PERSON
Unclassified	Unclassified	Unclassified	UU	7	William Teague
					19b. TELEPHONE NUMBER *(Include area code)* 228-688-4734

Measurements of hurricane induced high-frequency currents

Diane Bennett Fribance
Postoctoral Researcher, Ocean Sciences Branch
Naval Research Labs
Stennis Space Center, Mississippi, USA
diane.bennett.ctr@nrlssc.navy.mil

Hemantha W. Wijesekera, William J. Teague
Ocean Sciences Branch
Naval Research Labs
Stennis Space Center, Mississippi, USA

Abstract— **Hurricanes are powerful, energetic storms that can be fueled by warm ocean waters, while simultaneously driving transport and mixing under their path. Wind-driven mixing is an important mechanism for generating internal waves, and hurricanes are capable of generating particularly high levels of mixing. The internal waves in turn allow diapycnal mixing in the ocean, accelerating heat transfer from the near surface to deeper waters. This plays a role in global thermohaline circulation, affecting heat transfer and therefore density properties throughout the oceans. However, while the importance of internal waves is well established, direct measurements of hurricane-generated internal waves over the shelf and slope regions are scarce. As a result, the mechanisms for the generation of these waves by storms are poorly understood. Here we examine the high frequency response and generation of internal waves by Hurricane Ivan as it travelled over the continental shelf edge and slope in the Gulf of Mexico. Velocity data were collected as part of the Naval Research Laboratory's Shelf Energetics and Exchange Dynamics (SEED) experiment. Moorings consisted of Trawl Resistant Bottom Mounts (TRBMs) in the form of a dome-shaped pod known as a Barny due to its barnacle-like shape. The Barnies housed ADCPs and wave/tide gauges, and during the hurricane were subject to extreme current conditions. In particular, over the shelf where water depths are 60 – 90m and surface waves reached significant wave heights of at least 20 m, bottom currents generated by these waves were over 2 m s^{-1}. Despite these extreme conditions, which set the nearby National Data Buoy Center (NDBC) buoy 42040 adrift, the Barnies proved themselves to be robust, and continued to measure water velocity and pressure both during and after the hurricane's presence in the region. This was the first test of the instrumentation setup under these extreme conditions, and their survival allowed a unique suite of measurements to be made which would not have otherwise been possible.**

Two distinct responses were observed over the shallow shelf edge (~90 m) and the deep slope (~500 – 1000 m). During the forcing stage of the hurricane over the shelf edge, internal wave motions were found to be three-dimensional, and after the passage of the hurricane velocity fluctuations became primarily horizontal and lasted about 3 days. Over the slope, inertial (f) and super-inertial waves with frequencies of 2f, 3f, 4f and higher were excited by the hurricane. These super-inertial waves persisted for 2-4 days while near-inertial waves lasted more than a week. The super-inertial fluctuations were found near bottom over the slope (500 -1000 m) where kinetic energy levels were at least 25 times larger than the kinetic energy level during calm weather, indicating that turbulent dissipation rates and eddy diffusivities increased by two orders of magnitude. The storm-generated super-inertial motions have the potential to enhance mixing in the deeper part of the thermocline. The storm-generated super-inertial motions lead to mixing both along and across isopycnals, acting as a potential vector for warmer waters to reach the deep ocean.

Hurricane; High-frequency waves; Dissipation; Super-inertial

I. INTRODUCTION

Energy transfer from the ocean's surface to deeper waters is a subject of great importance, as mixing controls the rates of heat transfer within the global oceans and affects processes like thermohaline circulation that ultimately play a role in controlling climate. One proposed mechanism for the transfer of energy from the surface to the deep oceans is through wind-driven mixing, particularly during large storms [1,2]. Previous calculations indicate that wind-driven mixing, by generating internal gravity waves, may supply approximately one quarter of the total energy required to sustain global thermohaline circulation [3]. Unfortunately, direct observations of water velocities in the path of large storms such as hurricanes are extremely rare given the difficulty of predicting storm tracks and timing, and the challenges of sampling from a vessel during high wind and wave conditions. As a result, there is a limited collection of data sets available (e.g. [4,5,6,7]) and few prior observations provide high spatial and temporal resolution.

In 2004, as part of the Naval Research Laboratory's Shelf Energetics and Exchange Dynamics (SEED) program, fourteen moorings were deployed in the eastern Gulf of Mexico along the shelf break. Fig. 1 shows the location of these moorings, along with the path of Hurricane Ivan, which passed directly over the array. The low-frequency ocean response has been discussed elsewhere [8,9]. Here we present some novel results focused on observed energy levels at near-inertial (f) and super-inertial frequencies, both on the shelf and over the slope. The temporal and spatial scales of the hurricane-generated internal waves will be explored.

Naval Research Laboratory Stennis Space Center Contribution Number NRL/PP/7330/11/0769

0-933957-39-8 ©2011 MTS

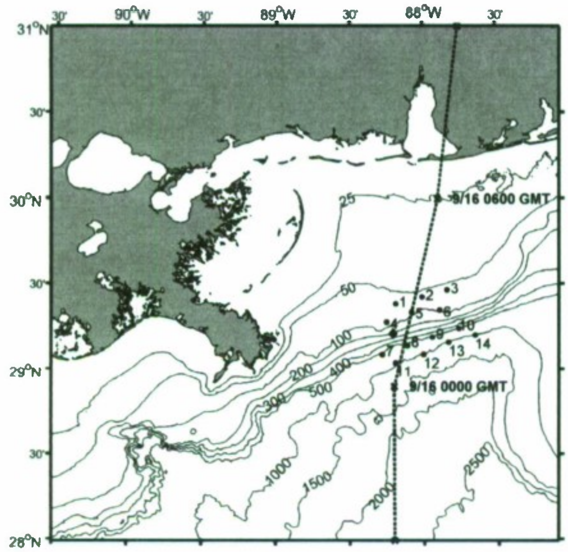

Figure 1. Location of SEED moorings, with bathymetry contours in meters. Dashed line shows path of Hurricane Ivan, as well as the time it passed over two waypoints in GMT. The diamond marks the location of the closest NDBC buoy.

II. Measurements and Methods

The fourteen ADCP moorings shown in Fig. 1 have been described in detail by Teague et al. [9]. They were deployed in early May, 2004, and recovered in November. Moorings M1-M3 were at 60 m depth, moorings M4-M6 were at 87-89 m depth, moorings M7-M10 were just beyond the shelf break in 510-530 m of water, and moorings M11-M14 were in water ranging from 1,016-1,038 m. The shelf stations, M1-M6, were equipped with Teledyne RD Instruments Workhorse ADCPs operating at 300 kHz which recorded an ensemble every 15 minutes and had a bin size of 2 m. The slope stations, M7-M14, utilized RD Instruments Long Ranger ADCPs operating at 75 kHz which recorded an ensemble every hour with a bin size of 10 m. While the ADCPs over the slope did not measure velocities below approximately 500 m, at the four deepest stations Aanderaa RCM9 Doppler current meters were deployed approximately 100 meters off the bottom, at 900 m depth.

The moorings were housed in Trawl-Resistant Bottom Mountings (TRBMs), and the mounting pods used are known as Barnies based on their barnacle-like shape. They are designed to not only be trawl-resistant, but also be deployable from small vessels, allow for recovery either by pop-up float or ballast release, and to be recoverable even if overturned [10]. The Barny has an outer cement ring, providing both protection and ballast, a buoyant main housing for a wave-tide gauge and two acoustic releases, and a central pop-up float containing the ADCP itself, all visible in Fig. 2a. Three recovery techniques, normal recovery (Fig. 2b) and emergency recoveries (Fig. 2c,d), are also illustrated.

All velocity data are pre-processed to remove surface contamination due to sidelobe effects. Horizontal velocities are all rotated 20 degrees counterclockwise to produce along-shelf and across-shelf coordinates. For filtered velocities, an eighth order digital elliptic filter is used [11], and is applied both forward and backward to avoid phase distortion. The inertial frequency (f) at the latitude of the moorings, 29° 15' N, is 0.041 cycles per hour (cph), which translates to a period of 24.5 hours. Both high-pass and low-pass versions of the filter bracket this and other frequencies of interest.

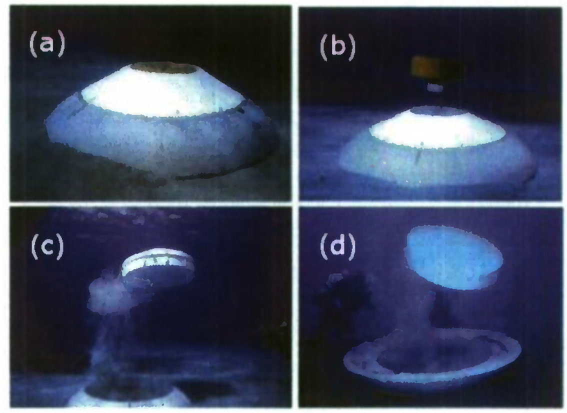

Figure 2: Barny TRBM (a) in deployment mode, (b) typical recovery by pop-up float, (c) emergency recovery by ballast drop, and (d) emergency recovery after being overturned. Images adapted from [10].

Energy spectra are calculated for some of the records as well. In cases where a depth range is examined, the mean of the velocities is determined before the spectral analysis. For power spectral density estimates, Welch's averaged, modified periodogram method is utilized [12]. In order to preserve as much frequency resolution as possible, the window length is the entire record in each case unless noted otherwise, and the form is a Hamming window.

III. Observations

A. High Frequency Response: Shelf

Ivan entered the Gulf of Mexico on 14 September 2004, and passed over the SEED array on September 16, year day 260, around 0000 UTC. Local winds were recorded by National Data Buoy Center (NDBC) buoy 42040. This buoy is located approximately between stations M4 and M7 (Fig. 1), and shows a maximum in wind speed just before midnight on September 15. The buoy broke loose during the hurricane's passage and as a result the signal is lost shortly after the peak wind event. The surface wind field over the mooring array during Ivan's passage was reconstructed (Fig. 3a) by combining wind data from the NDBC buoy and model winds from post storm wind analysis by Hurricane Research Division [13,14,15].

Panels b-d in Fig. 3 show the filtered water velocities in the along- shelf (u), across- shelf (v), and vertical (w) directions for station M5, a shelf station located directly under the hurricane's path with a total water depth of 89 meters. The velocities have been filtered to remove anything below a frequency of 0.20 cph, which is five times the local inertial frequency. There is a clear high-frequency velocity signal related to the passage of the hurricane in all three components of velocity. It is likely that these oscillations were high-frequency internal waves, supported by the local stratification. Measurements of temperature and salinity in the water column were not available

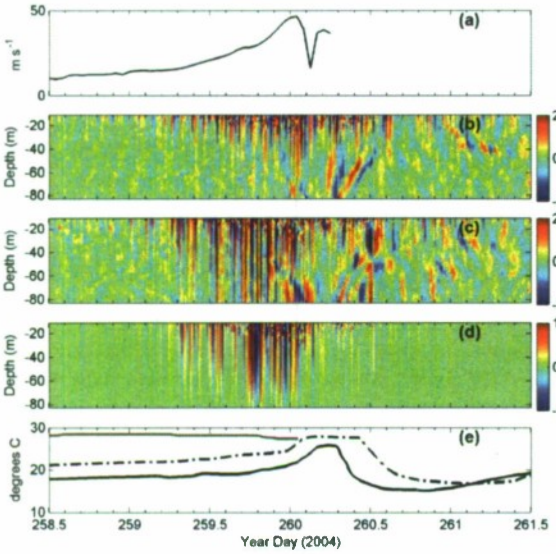

Figure 3: Wind speed (a), station M5 filtered velocities (cm s-1) across-shelf (b) along-shelf (c), and vertical (d), and water temperature (e). Only velocities at frequencies of $5f$ (0.2 cph) or greater are shown in b-d. Panel (e) shows surface temperature at the closest NDBC buoy (gray) and bottom temperature at stations M1 (black dashed) and M5 (black solid).

during the observations, and therefore the depth-averaged stratification was inferred from the temperature difference between sea surface (from the NDBC buoy) and bottom (M1-M6) temperatures (Fig. 3e). The estimated mean buoyancy frequency based on temperature difference alone on year day 259.25 was about 10 cph, indicating that the water column was strongly stratified at the early stage of the passage of Ivan. However, the temperature difference became small when Ivan crossed the array on year day 260, particularly at the shallower stations (represented by M1). The velocity sampling rate was 4 cph, and therefore only a fraction of high-frequency internal waves that could have been generated were recorded by the Barny moorings.

The onset of the high frequency oscillations somewhat preceded the peak wind speeds (Fig. 3). The strongest part of the signal, seen most clearly in the vertical velocities, lasted for approximately half a day, and the maximum duration of the higher frequency fluctuations was no more than one day. In general, the across-shelf velocities were the largest, and the vertical velocities were the smallest. However, in the case of these extremely high frequency oscillations all three velocity components were comparable in magnitude. These same effects are seen at all of the stations on the shelf, M1 through M6.

Another way to understand how the hurricane both increased overall energy levels and generated peaks at particular frequencies is to look at the energy spectra. Fig. 4 shows a power spectral density analysis of the near-surface velocities at station M5, separated into along-shelf (a), across-shelf (b) and vertical (c) components. Each velocity record is divided into pre-hurricane and hurricane-influenced segments. The pre-hurricane period is defined as the beginning of the record, from year day 128 through year day 258. For the horizontal velocities, the hurricane elevated inertial energy starting at year day 259, and energy levels returned to background levels at year day 270. This time frame was considered to be hurricane-influenced. In the case of the vertical velocities, the response was primarily high frequency and lasted through year day 261, so the spectral analysis was performed from year days 259 to 261. The power spectral density was calculated for each record, and for the pre-hurricane velocities a window the length of the hurricane-influenced period was applied to provide consistent resolution. In the horizontal velocity components, energy was overall higher at all frequencies during the hurricane's passage. The bottom panel of Fig. 4 shows clearly that the vertical velocities were enhanced primarily at high frequencies, greater than five times the inertial frequency.

B. Response at Multiples of the Inertial Frequency: Shelf

While the high frequency oscillations were most visible in the vertical velocities, over the shelf the lower frequency oscillations (near-inertial and super-inertial) were most prominent in the horizontal velocities, showing up as a primarily two-dimensional signal. The near-inertial currents at station M5 are shown in Fig. 5a and 5b. Unlike the high-frequency signal, which appeared before the arrival of the hurricane's peak winds and quickly dissipated after its passage, the near-inertial velocities increased in speed approximately as the hurricane passed over the mooring array at year day 260, and remained elevated for at least five days. These near-inertial and super-internal currents are highly baroclinic in nature, and are strongest near the surface and the bottom. Without measurements of temperature and salinity in the water column, it is difficult to evaluate the relationship between the thermocline's location and changes in near-inertial velocities as a function of depth.

In the filtered inertial velocities, the immediate horizontal response near the surface is clearly visible (Fig. 5a,b). This

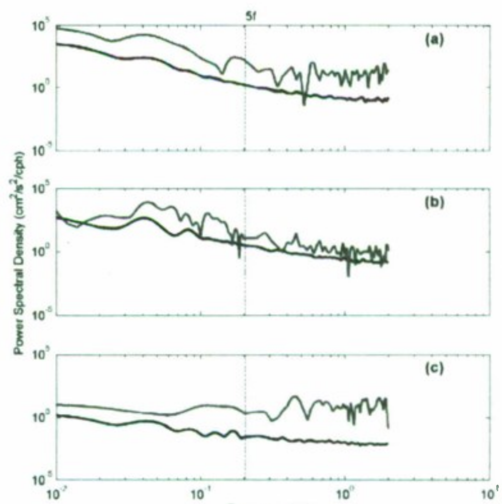

Figure 4: Depth-averaged power spectral density (PSD) estimates for along-shelf (a), across-shelf (b) and vertical (c) velocities. The PSD is calculated both for the pre-hurricane (black) and hurricane-influenced (gray) periods. Currents have been depth-averaged over the top 40 m, where the hurricane's influence is strongest (Figure 2). The vertical line marks five times the inertial frequency ($5f$).

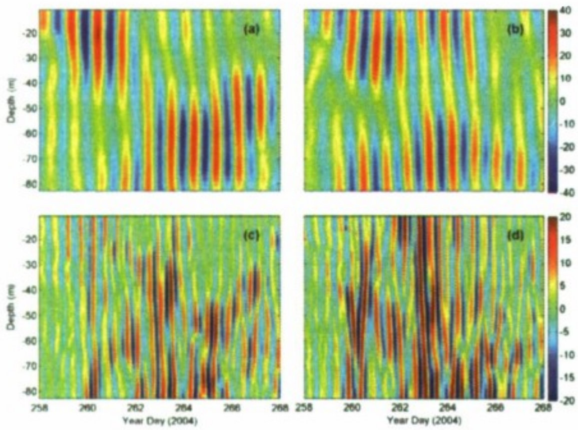

Figure 5: Station M5 filtered velocities (cm s-1), along-shelf (a,c) and across-shelf (b,d). Top panels show near-inertial velocities (along- and across- channel, respectively), and bottom panels show velocities between 2-4 times the inertial frequency.

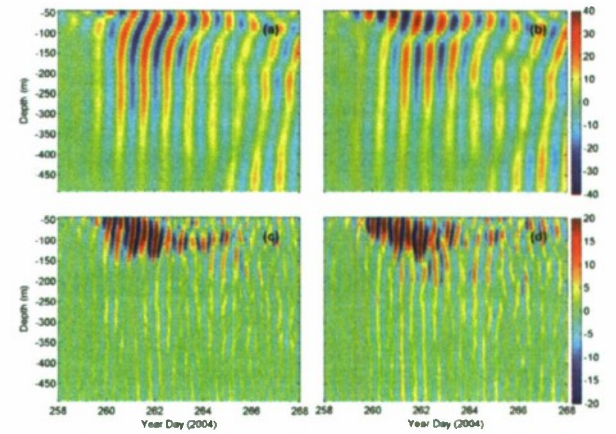

Figure 6: Station M11 filtered velocities (cm s-1), along-shelf (a,c) and across-shelf (b,d). Top panels show near-inertial velocities (along- and across- channel, respectively), and bottom panels show velocities between 2-4 times the inertial frequency.

initial amplification is followed by an increase in inertial velocities deeper in the water column, both along- and across-shelf, several days after the peak hurricane winds have passed. Inertial velocities at all depths have returned to background levels by year day 271. Complex demodulation reveals that the inertial currents are primarily rotating in the clockwise direction.

The super-inertial velocities at station M5 (Fig. 5c-d) are dominated by waves with frequencies in the range from twice the inertial frequency to four times the inertial frequency. These super-inertial currents are less energetic than the near-inertial currents, with maximum velocities approximately half as strong. However, they are also elevated over pre-hurricane levels, and the timing of the increased energy is similar to that at the inertial frequency, although energy returns to background levels somewhat sooner, around year day 269.

C. *Inertial and Super-Inertial Currents: Slope*

Eight SEED moorings were deployed over the continental slope, with four near the 500 meter isobath and the others along the 1,000 meter isobath. As a result of the increased water depths relative to the shelf stations, which were in approximately 500 meters of water, the hurricane response over the slope is closer to what might be expected in the deep ocean, away from coastal influence.

Stations M8 and M11 both lie directly under the hurricane's path, with M11 being the deeper of the two. At this station, and all of the slope stations, the response to the hurricane was primarily in the inertial band, and the very high frequency (>0.2 cph) response seen at the shallow stations was not observed here. It should be noted that the shallowest depths with velocity measurements at these stations is approximately 50 meters, so there may be higher frequency fluctuations near the surface that were unobserved.

In both horizontal directions, near-inertial oscillations were induced by the hurricane between the surface and approximately 300 meters, and the signal decayed with depth (Fig. 6). Inertial amplitudes (Fig. 6a,b) increased around year day 260, and remained elevated above background levels for approximately ten days. The across-shelf inertial response was more strongly surface intensified than the along-shelf response.

The response at the super-inertial frequencies (between two and four times the inertial, Figs. 6c,d) was intense over the shelf, but of shorter duration than the near-inertial response. It extended to approximately 150 meters depth, and lasted for three to five days. This is also a shorter duration than the near-inertial response over the shelf.

D. *Energy Changes with Depth over the Slope*

The internal wave activity over the slope both during and after the passage of Hurricane Ivan is of particular interest, as what happens at these depths is closely connected to mixing in the deep ocean. To see how energy is transmitted from the surface to near the sea floor over the slope, it is necessary to evaluate the changes in signal and energy as a function of depth.

The along-shelf and across-shelf power spectral density estimates over the slope are shown in Fig. 6, using stations M7 and M11 as examples. M7 is in shallower water (511 m) to the west, and M11 is in deeper water (1,016 m) to the east. For the 100 m and 450 m depths the spectra were calculated over a 100 m range and were then averaged. The 900 m record is from the Aanderaa current meter, located approximately 100 m off the sea floor at the same location as M11, and is a point measurement. The spectra are calculated using velocities between year day 258 and year day 268, which includes the forcing and relaxation stages of the hurricane response. It is immediately evident that at this deep station there is a lot of energy at twice the inertial frequency, particularly in the along-shelf direction (Fig. 7). This is most evident near the surface and the bottom, where the 2f signal is of comparable magnitude to the near-inertial signal. At 100 m there are also clear energy peaks at 3f and 4f. Overall energy levels are highest near the surface, but not much energy is lost between 450 and 900 m.

Another way to examine the energy pathways is to see how kinetic energy at specific frequencies evolves over time.

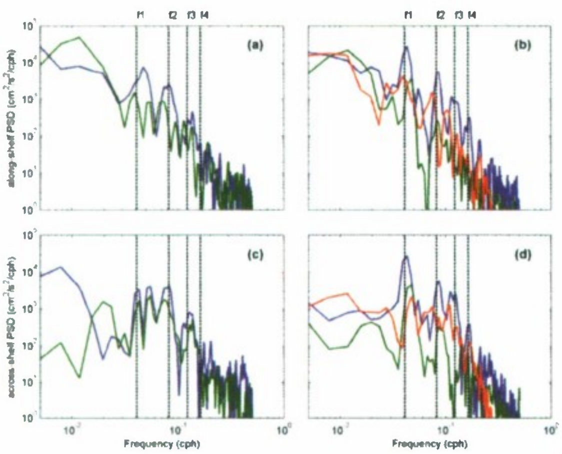

Figure 7: Spectra at station M7 (a,c) and M11 (b,d) in the along-shelf (a,b) and across-shelf (c,d) directions. Colors indicate depths, blue is a depth-average between 50-150m, green is 400-500m, and red is the 900m spectrum from the Aanderaa RCM9 Doppler current meter at M11. Dashed lines indicate f, 2f, 3f, and 4f frequencies.

Horizontal kinetic energy (HKE), $(u^2+v^2)/2$, can be calculated for specific depths and frequencies. The time-varying velocity signals were filtered to contain only the near-inertial (0.03 – 0.05 cph) and super-inertial (0.071 – 0.173 cph) frequencies. The super-inertial cutoffs were chosen to encompass energy between twice and four times the inertial frequency. Once the kinetic energy of the filtered velocities at each depth and location was calculated, the results were averaged to produce depth averages at 100 m and 450 m as described above, and averages over the shallow (M7-M10) and deep (M11-M14) slope.

The results of this analysis over the deeper slope stations are seen in Fig. 8. Near the surface (a), inertial and super-inertial HKE are of similar magnitude. At mid-depth (b), energy levels are initially similar, but during the relaxation stage inertial energy continues to increase while super-inertial energy levels are unchanged. Near bottom (c) super-inertial energy levels are higher than those at the near-inertial frequency. The shallower slope stations (M7 – M10) showed

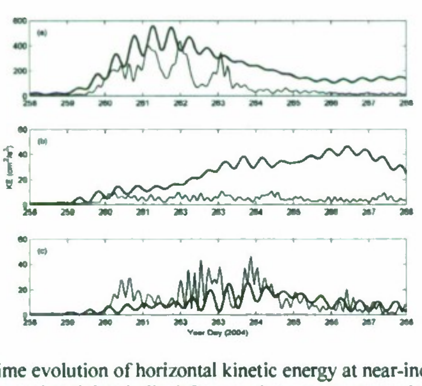

Figure 8: Time evolution of horizontal kinetic energy at near-inertial (thick line) and super-inertial (thin line) frequencies over the deep slope. Panels represent different water column depths: 50-150m (a), 400-500m (b), and 900m (c). Water depth is approximately 1000 m. Note differing vertical scale for panel (a).

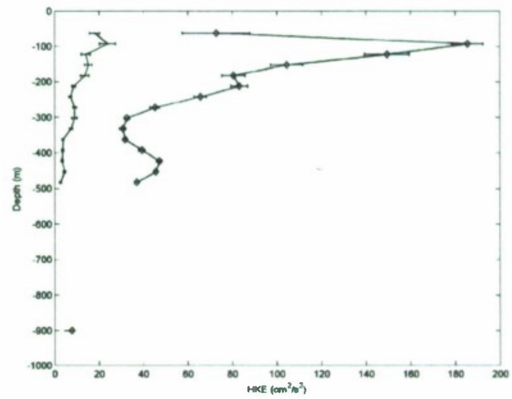

Figure 9: Horizontal kinetic energy in the near-inertial (◊) and super-inertial (•) bands between year day 261 and 262 as a function of depth over the deep slope. Error bars show standard error.

the same trends as a function of depth.

Shifting the focus to a specific period of time during the relaxation stage, there are some visible trends in the near- and super-inertial energy levels. Fig. 9 shows a time average of the near-inertial and super-inertial horizontal kinetic energy between year day 261 and year day 262, along with the standard error at each depth. Near the surface energy levels are high and variable, and there is a general trend of decreasing energy as a function of depth. Through most of the water column, there is more energy in the near-inertial band. However, 100 meters above the sea floor near-inertial and super-inertial energy levels become comparable. This is particularly interesting because the average super-inertial energy at this depth is higher than the average super-inertial energy at mid-depth.

IV. Discussion

The high-frequency response to the relatively fast-moving Hurricane Ivan was very different over the shelf from the response over the slope. While internal waves at the inertial frequency were generated over the shelf, there was also a very high frequency response throughout the water column that was visible in all three velocity components and that preceded the arrival of hurricane peak winds. Over the slope, the response was much more horizontal and baroclinic. There are clear signals at the near-inertial frequency as well as multiples of this frequency, implying that nonlinear mechanisms likely play an important role.

A. High-frequency internal waves over the shelf: Plausible Mechanism

Wave-like disturbances can be generated in a stratified shear flow by Kelvin-Helmoltz (K-H) instabilities [16]. K-H waves are generated when the Richardson number (Ri) becomes less than the critical value of 0.25. By assuming a constant temperature gradient, and using temperature to drive density calculations, we estimated the depth-averaged Ri. Using this, we noted that the formation of high-frequency waves was well correlated with below critical values of Ri.

Prior to the passage of Ivan, the water column was well stratified: for example, on year day 259, the temperature difference between the shelf bottom (at M1-M6) and the surface (at NDBC buoy) was 6-8°C, which corresponds to a buoyancy frequency of about 10 cph with depth averaged Ri ~0.5-1. The advancing storm generated highly sheared cross-shelf flow: on-shore current near the surface and off-shore flow near the bottom [8]. The stratification decreased as the wind-driven coastal flow became strong, and Ri dropped below critical on year day 259.5 which coincides with the onset of the high frequency oscillations. For simplicity, the observed cross-shelf current can be treated as a bounded shear flow (e.g., 4.4c in [16]) which supports an unlimited number of unstable K-H modes, similar to the observed high-frequency internal waves in multiple frequency bands (Fig. 4).

B. *Mixing over the slope*

Previous work by Niwa and Hibiya [17] predicted that a hurricane moving at a constant speed over the ocean would lead to internal waves at twice and three times the inertial frequency, generated through nonlinear effects. They also predicted that waves at twice the inertial frequency could contain more energy than near-inertial waves in areas away from the hurricane track. This result was confirmed by Zedler [18] who also generated internal waves at twice the inertial frequency in her model when hurricane conditions were simulated, although the proposed mechanisms differed. The results here suggest that these internal waves with a frequency of 2f are being generated near the surface (as seen in Fig. 6), and the presence of energy at twice the inertial frequency at 900 m over the slope is in accordance with the model results of Danioux and Klein [19]. Without stratification, we cannot accurately separate out the baroclinic modes to test whether it is the low modes producing the 2f peak (as proposed by Danioux and Klein), but the observations are consistent with the model predictions based on the similarities between modeled and observed energy spectra.

One of the key results from Danioux et al. [20] involves mesoscale eddies. Both their numerical and analytic models generated waves at the 2f frequency due to the presence of mesoscale eddies, which are believed to destabilize the near-inertial motions, reduce their horizontal scales, and allow energy to propagate vertically. Baroclinic instabilities are generated in their model by the presence of a large-scale jet, and result in an rms Rossby number Ro=0.10 (where $Ro=\sqrt{\langle\zeta^2\rangle}f_0^{-1}$, if ζ is the eddy relative vorticity and f_0 is the Coriolis frequency in the center of the mooring array), once the model has reached equilibrium. An analysis of the relative vorticity over the scale of our entire mooring array, which has horizontal scales of approximately 60 km along-shelf and 12 km over the slope across-shelf, revealed an rms Rossby number during low winds of approximately 4. Choosing the low-wind period minimizes wind-driven eddy generation mechanisms, leaving a baseline relative vorticity field that was present when Ivan approached the region. The strong relative vorticity and resulting high Rossby number indicate the presence of mesoscale eddies, shown to be a potential mechanism for the vertical propagation of energy [20].

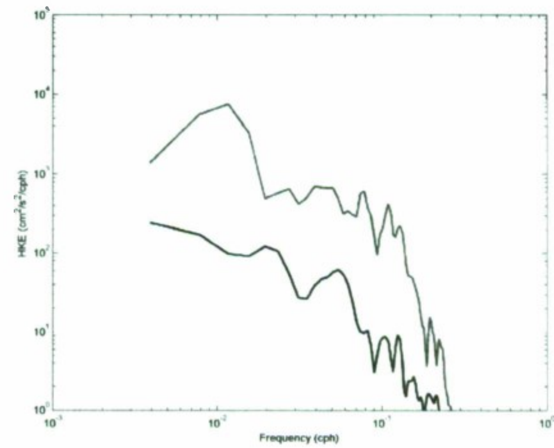

Figure 10: Horizontal kinetic energy from velocities averaged over four deep current meters along the continental slope. Black line is during a 10-day low wind period (year day 201-211) and gray line is during hurricane Ivan (year days 258-268).

The relative energy levels during a low wind period and during the hurricane's passage are related to energy dissipation rates during these same time periods. Horizontal kinetic energy at 900m depth over the slope was calculated for a calm period (year day 201-211) and the time surrounding the hurricane (year day 258-268), as shown in Fig. 10. During the ten day period surrounding the hurricane, kinetic energy integrated above the inertial frequency is 26.7 times higher than during the low-wind period. At first order, the dissipation rate (ε) is proportional to E^2N^2, where N is the buoyancy frequency and E is the internal wave energy of the f to N frequency band (e.g., [21]). It is unlikely that the background stratification in the deep ocean would change significantly during calm and stormy weather, and therefore the dissipation rates during the hurricane are potentially two orders of magnitude higher than rates during low-wind periods. This would help to explain how these high energy events can cause localized mixing and dissipation rates to be elevated enough to contribute significantly to the heat and mass balances on regional scales, even though they are of limited extent and duration.

V. SUMMARY

Hurricane Ivan passed directly over the SEED array of moorings, providing a unique and extensive set of velocity measurements in the wake of a hurricane. In particular, this provided a unique opportunity to see how closely the observed high-frequency internal waves correspond to predictions based on theory indicating that forcing at high wind speeds should generate near-inertial waves as well as those at multiples of the inertial frequency, and particularly at 2f.

The shelf response, observed in all three velocity components at the onset of Ivan, was highly super-inertial (5f and above), and lasted approximately half a day to one day. Energy was elevated to some extent at all frequencies as the hurricane passed over the shelf, but there was a distinct high-frequency response. During the arrival and after the passage of Ivan, the response was both near-inertial and super-inertial at two to four times the inertial frequency, lasting several days.

The near-inertial waves reached maximum velocities later than the super-inertial waves, and persisted for at least five days. Richardson number calculations at the shelf stations, which were initially stratified, indicate that mixing likely generated K-H instabilities. These instabilities are a likely source of the observed high-frequency oscillations.

Over the slope, near-inertial waves were the strongest, lasting approximately ten days and concentrated in the upper 300 meters. Similar to the shelf response, over the slope at super-inertial frequencies the response was shorter (3-5 days) and shallower (~150 m). Near the surface, energy peaks were indeed observed at multiples of the inertial frequency (2f, 3f, 4f). At near-surface depths, kinetic energy is initially of similar magnitude at near- and super-inertial frequencies, but at mid-depth during the relaxation stage kinetic energy is higher at near-inertial frequencies. At depth, super-inertial energy levels are higher than the near-inertial energy levels.

The observations of near-surface peaks in energy at twice the inertial frequency over the slope are also consistent with model predictions, although proposed mechanisms cannot be tested without information about stratification. The hurricane led to kinetic energy levels at and above the inertial frequency over the slope that were a factor of 27 higher than during low-wind conditions, indicating that dissipation rates during the hurricane may be elevated by two orders of magnitude relative to calm conditions.

ACKNOWLEDGMENT

This work was performed while the corresponding author held a National Research Council Research Associateship Award at the Naval Research Laboratory (NRL). The data were collected as part of the NRL's basic research project Slope to Shelf Energetics and Exchange Dynamics (SEED).

REFERENCES

[1] Niwa, Y. and T. Hibiya, 1999: Response of the deep ocean internal wave field to traveling midlatitude storms as observed in long-term current measurements. *J. Geophys. Res.*, **104 (C5)**, 10981-10989.

[2] Liu, L. L., W. Wang, and R. X. Huang, 2007: The Mechanical Energy Input to the Deep Ocean Induced by Tropical Cyclones. *J. Geophys. Res.*, **38**, 1253-1266.

[3] Alford, M. H., 2003: Redistribution of energy available for ocean mixing by long-range propagation of internal waves. *Nature*, **423**, 2003.

[4] Brink, K. H., 1989: Observations of the response of thermocline currents to a hurricane. *J. Phys. Oceanogr.*, **19**, 1017-1022.

[5] Brooks, D. A., 1983: the wake of Hurricane Allen in the western Gulf of Mexico. *J. Phys. Oceanogr.*, **13**, 117-129.

[6] Dickey, T., D. Frye, H. Jannasch, E. Boyle, D. Manov, D. Sigurdson, J. McNeil, M. Stramska, A. Michaels, N. Nelson, D. Siegel, G. Change, J. Wu, and A. Knap, 1998: Initial results from the Bermuda Testbed Mooring program. *Deep Sea Res. Part I*, **45**, 771-794.

[7] Zedler, S. E., T.D. Dickey, S.C. Doney, J.F. Price, X. Yu, and G.L. Mellor, 2002: Analysis and Simulations of the Upper Ocean's Response to Hurricane Felix at the Bermuda Testbed Mooring Site: 13-23 August 1995. *J. Geophys. Res.*, **107 (C12)**, 3232.

[8] Mitchell, D. A., W. J. Teague, E. Jarosz, and D. W. Wang, 2005: Observed currents over the outer continental shelf during Hurricane Ivan. *Geophys. Res. Lett.*, **32**, L11610 , doi:10.1029/2005GL023014.

[9] Teague, W.J., E. Jarosz, D.W. Wang, and D.A. Mitchell, 2007: Observed Oceanic Response over the Upper Continental Slope and Outer Shelf during Hurricane Ivan. *J. Phys. Oceanogr.*, **37**, 2181-2206.

[10] Perkins, H. F. Strobel and L. Gualdesi, 2000: The Barny Sentinel Trawl-Resistant ADCP Bottom Mount: Design, Testing, and Application. *IEEE J. Oceanic Eng.*, **25 (4)**, 430-436.

[11] Parks, T. W. and C. S. Burrus, 1987: *Digital Filter Design* (Sect. 7.3.3). Wiley, New York.

[12] Welch, P. D., 1967: The Use of Fast Fourier Transform for the Estimation of Power Spectra: A Method Based on Time Averaging Over Short, Modified Periodograms, *IEEE Trans. Audio Electroacoust.*, **AU-15**, 70-73.

[13] Powell, M. D., S. H. Houston, L. R. Amat, and N. Morisseau-Leroy, 1998: The HRD real-time hurricane wind analysis system. *J. Wind Eng. Ind. Aerodyn.*, **77&78**, 53-64.

[14] Wang, D. W., D. A. Mitchell, W. J. Teague, E. Jarosz, and M. S. Hulbert, 2005: Extreme waves under Hurricane Ivan, *Science*, **309**, 896.

[15] Atlantic Oceanographic and Meteorological Laboratory, cited 2011: Surface Wind Analysis. [Available online at http://www.aoml.noaa.gov/hrd/data_sub/wind.html.]

[16] Drazin, P. G. and W. H. Reid, 1981: *Hydrodynamic Stability.* 1st ed. Cambridge University Press, 536 pp.

[17] Niwa, Y. and T. Hibiya, 1997: Nonlinear processes of energy transfer from traveling hurricanes to the deep ocean internal wave field. *J. Geophys. Res.*, **102 (C6)**, 12469-12477.

[18] Zedler, S. E., T.D. Dickey, S.C. Doney, J.F. Price, X. Yu, and G.L. Mellor, 2002: Analysis and Simulations of the Upper Ocean's Response to Hurricane Felix at the Bermuda Testbed Mooring Site: 13-23 August 1995. *J. Geophys. Res.*, **107 (C12)**, 3232.

[19] Danioux, E. and P. Klein, 2008: A Resonance Mechanism Leading to Wind-Forced Motions with a 2*f* Frequency. *J. Phys. Oceanogr.*, **38**, 2322-2329.

[20] Danioux, E., P. Klein, and P. Rivière, 2008: Propagation of wind Energy into the Deep Ocean through a Fully Turbulent Mesoscale Eddy Field. *J. Phys. Oceanogr.*, **38**, 2224-2241.

[21] Gregg, M. C., 1989: Scaling Turbulent Dissipation in the Thermocline. *Journal of Geophysical Research*, **94 (C7)**, 9686-9